

S -wave contributions to the $B_{(s)} \rightarrow \chi_{c1}(\pi\pi, K\pi, KK)$ decays

Meng-Kun Jia¹, Chao-Qi Zhang¹, Jia-Ming Li¹, and Zhou Rui^{1*}

¹College of Sciences, North China University of Science and Technology, Tangshan 063009, China
(Dated: July 30, 2021)

We make a detailed study of the three-body decays $B_{(s)} \rightarrow \chi_{c1}hh'$, where $h^{(\prime)}$ is either a pion or kaon, by taking into account the S -wave states in the hh' invariant mass distribution within the perturbative QCD approach. The two meson distribution amplitudes (DAs) are introduced to capture the strong interaction related to the production of the hh' system. We calculate the branching ratios for the S -wave components and observe large values of order 10^{-4} for some Cabibbo-favored decays, which are accessible to the LHCb and Belle II experiments. The obtained branching ratio $\mathcal{B}(B \rightarrow \chi_{c1}K_0^*(1430)(\rightarrow K^+\pi^-)) = (5.1_{-0.8}^{+0.6}) \times 10^{-5}$ consistent with the data from Belle within errors. Moreover, we also predict the differential distributions in the hh' invariant mass for the decays under consideration, which await the future experimental test. In addition, the corresponding $\chi_{c1}(2P)$ channels are also investigated, which are helpful to clarify the nature of the $X(3872)$ state.

PACS numbers: 13.25.Hw, 12.38.Bx, 14.40.Nd

I. INTRODUCTION

B meson decays to final states containing a charmonium meson have played a crucial role in the observation of CP violation in the weak interactions of quarks and provided powerful probes of the strong interaction in a heavy meson system. In particular, the χ_{c1} modes, which are allowed under the factorization hypothesis, are found to be a comparison of production rates with respect to the similar J/ψ processes [1]. Studying the production of χ_{c1} meson and its radial excited states in B meson decays will help to shed light on the production mechanisms in the exclusive charmonium B decays.

Two-body decays of $B \rightarrow \chi_{c1}\pi$ [2, 3] and $B \rightarrow \chi_{c1}K^{(*)}$ [4–6] have been observed and well measured by several collaborations. Also, some multibody decay modes, such as $B^0 \rightarrow \chi_{c1}K^+\pi^-$ [7], $B_s \rightarrow \chi_{cJ}K^+K^-$ [8], and $B \rightarrow \chi_{c1}\pi\pi K$ [9], were observed, for which one can search for charmonium or charmoniumlike exotic states in the pion-charmonium invariant mass distribution. For example, the narrow exotic resonance $X(3872)$ was discovered in the $J/\psi\pi^+\pi^-$ invariant mass spectrum produced in $B \rightarrow J/\psi\pi^+\pi^-K$ decays by the Belle experiment [10], and later confirmed by multiple other experiments [11–14]. In addition, the $X(3872)$ state was also observed in $B \rightarrow X(3872)K\pi$ decays [15]. Its quantum number assignment have been identified to be $J^{PC} = 1^{++}$ [16–18], suggesting it may be the typical $\chi_{c1}(2P)$ charmonium state in the quark model scenario. However, its mass (3871.69 ± 0.17 MeV), narrow width ($\Gamma < 1.2$ MeV) [1], and the isospin violating decay chain $X(3872) \rightarrow J/\psi\rho^0 \rightarrow J/\psi\pi^+\pi^-$ [16–22] imply that it may not be a simple $c\bar{c}$ charmonium state. Results from recent LHCb studies [23–25] also support it may have further mystery substructure beyond the conventional charmonium model. Popular interpretations, including $\chi_{c1}(2P)$ state, tetraquark, molecular state, admixture state, $c\bar{c}g$ hybrid state, and vector glueball, have been proposed [26–43], which means the question of its internal structure remain open. A more detailed discussions of the current knowledge of the $X(3872)$ properties can be found in Ref. [44] and references therein.

B meson two-body decays into a final states containing $\chi_{c1}(1P, 2P)$ state have generated much theoretical discussions [45–53]. In particular, the authors of Ref. [52] analyzed the two-body $B \rightarrow \chi_{c1}(1P, 2P)$ decays in QCD factorization by treating charmonia as nonrelativistic bound states. They found that the $B \rightarrow \chi_{c1}(2P)K$ decay rate can be comparable to that of $\chi_{c1}(1P)$ mode and argued that $X(3872)$ may be dominated by the $\chi_{c1}(2P)$ charmonium but mixed with a $D^0\bar{D}^{*0}/D^{*0}\bar{D}^0$ molecule state. In Ref. [53], the branching ratio of the $B \rightarrow X(3872)K$ was calculated in the PQCD approach, by assuming $X(3872)$ to be a regular $\chi_{c1}(2P)$ charmonium state. The obtained number is larger than the current upper bound set by Belle [54] within the error bar, which indicate a pure charmonium assignment for $X(3872)$ is not suitable. Further studies should be carried out in other exclusive decays to clarify its inner structure, especially in the three-body $B \rightarrow \chi_{c1}(2P)hh'$ decays, which are still lacking in the literature to date.

In this consideration, we study the three-body decays $B \rightarrow \chi_{c1}hh'$ with $h, h' = \pi, K$ within the framework of

*Electronic address: jindui1127@126.com

perturbative QCD (PQCD), where χ_{c1} is used to denote the $\chi_{c1}(1P)$ and $\chi_{c1}(2P)$ collectively. The latter could help to clarify the nature of the $X(3872)$ since $\chi_{c1}(2P)$ may be one of possible assignments for $X(3872)$ as mentioned above. Here we put the focus on the hh' pair originating from a S -wave configuration, while the subjects related to the crossed-channel such as $\chi_{c1}h^{(\prime)}$ and other higher partial wave are outside the ambit of the present analysis. For recent works applying triangle singularities to interpreting several charmoniumlike structures in the $X_{cc}\pi^+$ invariant mass distributions of $\bar{B}^0 \rightarrow X_{cc}K^-\pi^+$ with $X_{cc} = J/\psi, \psi(2S), \chi_{c1}$, we refer the reader to Refs. [55–57].

The PQCD approach has been successfully applied to various three-body charmonium decays of B meson to investigate the contributions of the resonances involved [58–65]. The method has also been extended to the four-body charmless hadronic B meson decays very recently [66, 67]. Within the quasi-two-body approximation, we assume two light final-state mesons h and h' move almost parallelly for producing a resonance. The associated final-state interactions inside hh' pair are parametrized into the nonperturbative two meson distribution amplitudes (DAs) [68–74]. That is, three-body processes are assumed to proceed predominantly via one intermediate state which strongly decay into two light meson. The corresponding decay amplitude can be conceptually written as the convolution of all the perturbative and nonperturbative objects

$$\mathcal{A} = \Phi_B \otimes H \otimes \Phi_{hh'} \otimes \Phi_{\chi_{c1}}, \quad (1)$$

where Φ_B and $\Phi_{\chi_{c1}}$ are the nonperturbative B meson and charmonium DAs, respectively. The two meson DA $\Phi_{hh'}$ absorbs the nonperturbative dynamics of the hadronization processes in the hh' system. The hard kernel H , similar to the case of two-body decays, includes the leading-order contributions plus the vertex corrections. As pointed in Refs. [49, 52] that the infrared divergences arising from vertex corrections cancel in the $B \rightarrow \chi_{c1}$ decay as in the case of $B \rightarrow J/\psi$. Therefore, the vertex corrections obtained in QCDF can be applied to PQCD without introducing any extra parton transverse momenta [60].

The paper is organized as follows. After the Introduction, we present our model kinematics and describe the S -wave DAs in $\pi\pi$, $K\pi$, and KK pairs, respectively. In Sec. III, we make predictions of the branching ratio and the differential distribution for each S -wave component in the considered three-body decays. In final section, we give discussions and the conclusion. Some technical details are relegated to the Appendix.

II. KINEMATICS AND THE S -WAVE TWO MESON DISTRIBUTION AMPLITUDES

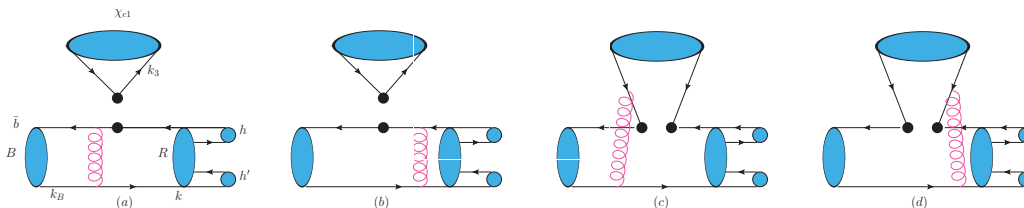


FIG. 1: Feynman diagrams for the $B_{(s)} \rightarrow \chi_{c1}R(\rightarrow hh')$ decays at the leading-order approximation, where the symbol \bullet denotes the insertion of effective weak interaction.

Consider the quasi-two-body process $B_{(s)} \rightarrow \chi_{c1}R(\rightarrow hh')$, whose leading order diagrams are shown in Fig. 1. In the rest frame of the $B_{(s)}$ meson, we assume the final state charmonium is moving along the direction of $v = (0, 1, \mathbf{0}_T)$ while the meson pair is along $n = (1, 0, \mathbf{0}_T)$, with n and v are two lightlike vectors in the lightcone coordinates. Then the $B_{(s)}$ meson momentum p_B , the χ_{c1} meson momentum p_3 , and the meson pair momentum p can be parametrized as [75]

$$p_B = \frac{M}{\sqrt{2}}(1, 1, \mathbf{0}_T), \quad p_3 = \frac{M}{\sqrt{2}}(g^-, g^+, \mathbf{0}_T), \quad p = \frac{M}{\sqrt{2}}(f^+, f^-, \mathbf{0}_T), \quad (2)$$

where the variables

$$\begin{aligned} f^\pm &= \frac{1}{2}(1 + \eta - r^2 \pm \sqrt{(1 - \eta)^2 - 2r^2(1 + \eta) + r^4}), \\ g^\pm &= \frac{1}{2}(1 - \eta + r^2 \pm \sqrt{(1 - \eta)^2 - 2r^2(1 + \eta) + r^4}), \end{aligned} \quad (3)$$

with the mass ratio $r = m/M$ and $m(M)$ is the mass of the charmonium (B meson). The factor η is defined as $\eta = \omega^2/M^2$ with ω being the invariant mass of the meson pair satisfying $p^2 = \omega^2$. The meson momenta p_1 and p_2 inside meson pair, obeying momentum conservation $p = p_1 + p_2$ and the on-shell conditions $p_{1,2}^2 = m_{1,2}^2$, one can derive them

$$\begin{aligned} p_1 &= \left(\frac{M}{\sqrt{2}} \left(\zeta + \frac{r_1 - r_2}{2\eta} \right) f^+, \frac{M}{\sqrt{2}} \left(1 - \zeta + \frac{r_1 - r_2}{2\eta} \right) f^-, \mathbf{p}_T \right), \\ p_2 &= \left(\frac{M}{\sqrt{2}} \left(1 - \zeta - \frac{r_1 - r_2}{2\eta} \right) f^+, \frac{M}{\sqrt{2}} \left(\zeta - \frac{r_1 - r_2}{2\eta} \right) f^-, -\mathbf{p}_T \right), \end{aligned} \quad (4)$$

with the mass ratios $r_{1,2} = m_{1,2}^2/M^2$. ζ is the meson momentum fraction up to corrections from the meson masses [66]. By use of the on-shell conditions $p_{1,2}^2 = m_{1,2}^2$, the transverse momentum \mathbf{p}_T can be written as

$$|\mathbf{p}_T|^2 = \omega^2 \left[\zeta(1 - \zeta) + \frac{(r_1 - r_2)^2}{4\eta^2} - \frac{r_1 + r_2}{2\eta} \right]. \quad (5)$$

In the hh' rest frame, the three-momenta of the final states h and charmonium are written as

$$|\vec{p}_1| = \frac{\sqrt{\lambda(\omega^2, m_1^2, m_2^2)}}{2\omega}, \quad |\vec{p}_3| = \frac{\sqrt{\lambda(M^2, m^2, \omega^2)}}{2\omega}, \quad (6)$$

respectively, with the Källén function $\lambda(a, b, c) = a^2 + b^2 + c^2 - 2(ab + ac + bc)$. To evaluate the hard kernels, the following parametrization for the valence quark momenta labeled by k_B , k_3 , and k in Fig. 1 is useful:

$$k_B = \left(0, \frac{M}{\sqrt{2}} x_B, \mathbf{k}_{BT} \right), \quad k_3 = \left(\frac{M}{\sqrt{2}} g^- x_3, \frac{M}{\sqrt{2}} g^+ x_3, \mathbf{k}_{3T} \right), \quad k = \left(\frac{M}{\sqrt{2}} f^+ z, 0, \mathbf{k}_T \right), \quad (7)$$

with the parton momentum fractions x_B, x_3, z and the corresponding transverse momenta $\mathbf{k}_{BT}, \mathbf{k}_{3T}, \mathbf{k}_T$.

The light-cone hadronic matrix element for a $B_{(s)}$ meson is decomposed as [76]

$$\Phi_{B_{(s)}}(x, b) = \frac{i}{\sqrt{2N_c}} [(\not{p}_B + M) \gamma_5 \phi_{B_{(s)}}(x, b)], \quad (8)$$

with b being the conjugate variable of the parton transverse momentum k_T , and N_c denoting the number of colors. We here only consider the leading Lorentz structure, while other subleading contributions [77, 78] are negligible within the accuracy of the current work. For the $B_{(s)}$ meson DAs, we adopt the conventional form [76, 79],

$$\phi_{B_{(s)}}(x, b) = N_{B_{(s)}} x^2 (1 - x)^2 \exp \left[-\frac{x^2 M^2}{2\omega_{B_{(s)}}^2} - \frac{\omega_{B_{(s)}}^2 b^2}{2} \right], \quad (9)$$

with the shape parameter $\omega_B = 0.40 \pm 0.04$ GeV for $B_{u,d}$ mesons and $\omega_{B_s} = 0.48 \pm 0.05$ GeV for a B_s meson [80]. The normalization constant $N_{B_{(s)}}$ is related to the $B_{(s)}$ meson decay constant $f_{B_{(s)}}$ via the normalization

$$\int_0^1 \phi_{B_{(s)}}(x, b=0) dx = \frac{f_{B_{(s)}}}{2\sqrt{2N_c}}. \quad (10)$$

For more alternative models of B meson DA, one can refer to [81–83].

The distribution amplitudes of χ_{c1} , defined via the nonlocal matrix element, have been derived in Ref [84]. The longitudinal polarization component is given by

$$\Phi_{\chi_{c1}} = \frac{1}{\sqrt{2N_c}} \gamma_5 \not{L} (m \chi_L(x) + \chi_t(x) \not{p}_3), \quad (11)$$

with the longitudinal polarization vector $\epsilon_L = \frac{1}{\sqrt{2}\eta}(-g^-, g^+, \mathbf{0}_T)$. The twist-2 and twist-3 DAs are collected as follows:

$$\begin{aligned}\chi_L(x) &= \frac{f_{\chi_{e1}}}{2\sqrt{6}} N_L x(1-x)\mathcal{T}(x), \\ \chi_t(x) &= \frac{f_{\chi_{e1}}^\perp}{2\sqrt{6}} \frac{N_T}{6} (2x-1)[1-6x+6x^2]\mathcal{T}(x),\end{aligned}\quad (12)$$

where $f_{\chi_{e1}}^{(\perp)}$ is the vector (tensor) decay constants. The coefficients $N_{L,T}$ satisfy the normalization conditions [84, 85]

$$\int_0^1 N_L x(1-x)\mathcal{T}(x)dx = 1, \quad \int_0^1 N_T x(1-x)(2x-1)^2\mathcal{T}(x)dx = 1. \quad (13)$$

The function $\mathcal{T}(x)$ can be extracted from P -wave Schrödinger states for a Coulomb potential. Its explicit expression for $1P$ state can be found in Ref. [84, 86], while that of $2P$ state will be derived in the appendix.

The light-cone matrix element for a S -wave meson pair is decomposed, up to the twist 3, into [58, 87]

$$\Phi_{hh'}^{S-wave} = \frac{1}{\sqrt{2N_c}} [P\phi_S^0(z, \omega) + \omega\phi_S^s(z, \omega) + \omega(\not{n}\not{\phi} - 1)\phi_S^t(z, \omega)] P_l(2\zeta - 1), \quad (14)$$

where the Legendre polynomials $P_l(2\zeta - 1) = 1$ for S -wave component. The two-meson DAs are parametrized as

$$\begin{aligned}\phi_S^0(z, \omega) &= \begin{cases} \frac{9F_{hh'}(\omega)}{\sqrt{2N_c}} a_{hh'} z(1-z)(1-2z), & hh' = \pi\pi, KK, \\ \frac{3F_{hh'}(\omega)}{\sqrt{2N_c}} z(1-z) \left[\frac{1}{\mu_S} + B_1 3(1-2z) + B_3 \frac{5}{2}(1-2z)(7(1-2z)^2 - 3) \right], & hh' = K\pi, \end{cases} \\ \phi_S^s(z, \omega) &= \frac{F_{hh'}(\omega)}{2\sqrt{2N_c}}, \\ \phi_S^t(z, \omega) &= \frac{F_{hh'}(\omega)}{2\sqrt{2N_c}} (1-2z),\end{aligned}\quad (15)$$

with the Gegenbauer moments $a_{\pi\pi} = 0.2 \pm 0.2$ [58], $a_{KK} = 0.80 \pm 0.16$ [62], $B_1 = -0.57 \pm 0.13$ and $B_3 = -0.42 \pm 0.22$ [88, 89]. Except for the twist-2 DA of the $K\pi$ pair, others are set to the asymptotic forms since the coefficients in the Gegenbauer expansion of the two meson DAs are poorly known at the moment.

The time-like scalar form factors $F_{hh'}(\omega)$, which absorbs the elastic rescattering effects in a final-state meson pair, are parameterized in different forms according to different meson pairs. Let's begin with the pion pair first. There are two intriguing light scalar resonances $f_0(500)$ and $f_0(980)$ below or near 1 GeV, which can couple to $\pi^+\pi^-$. Their internal structures were quite controversial [90–93]. The LHCb collaboration observed a peak for the $f_0(980)$ in the $B_s^0 \rightarrow J/\psi\pi^+\pi^-$ decay, while that of $f_0(500)$ is not seen [94]. On the contrary, in the corresponding B_s decay, a signal is seen for the $f_0(500)$ production, but no visible trace for $f_0(980)$ production. Therefore, in this work, we assume the $f_0(500)$ and $f_0(980)$ enter into the non-strange and strange scalar form factors, respectively. The former contribute dominantly in the B^0 decay, while the latter should feature mainly in the B_s^0 mode.

Including higher resonances, the strange scalar form factor can be described as the coherent sum of three scalar resonances $f_0(980)$, $f_0(1500)$, and $f_0(1790)$, which have been widely employed in the PQCD studies of the $B_s \rightarrow (J/\psi, \psi(2S), \eta_c, \eta_c(2S))\pi\pi$ decays [58, 95–97]. Explicitly, we have [58]

$$\begin{aligned}F_{\pi\pi}^{s\bar{s}}(\omega) &= \frac{c_1 m_{f_0(980)}^2 e^{i\theta_1}}{m_{f_0(980)}^2 - \omega^2 - im_{f_0(980)}(g_{\pi\pi\rho\pi\pi} + g_{KK\rho KK})} \\ &+ \frac{c_2 m_{f_0(1500)}^2 e^{i\theta_2}}{m_{f_0(1500)}^2 - \omega^2 - im_{f_0(1500)}\Gamma_{f_0(1500)}(\omega^2)} \\ &+ \frac{c_3 m_{f_0(1790)}^2 e^{i\theta_3}}{m_{f_0(1790)}^2 - \omega^2 - im_{f_0(1790)}\Gamma_{f_0(1790)}(\omega^2)},\end{aligned}\quad (16)$$

where c_i and θ_i , $i = 1, 2, 3$, are the corresponding weight coefficients and phases of the resonances with the parameter values of Ref. [58]. m_{f_0} is the nominal mass of the resonance. $\Gamma_{f_0}(\omega)$, the mass-dependent width, is defined as in the case of a scalar resonance

$$\Gamma_{f_0}(\omega) = \Gamma_{f_0} \frac{m_{f_0}}{\omega} \left(\frac{\omega^2 - 4m_\pi^2}{m_{f_0}^2 - 4m_\pi^2} \right)^{\frac{1}{2}}, \quad (17)$$

where Γ_{f_0} is the partial width of the resonance. Different from $f_0(1500)$ and $f_0(1790)$ resonances described usually by Breit-Wigner (BW) model, $f_0(980)$ is parameterized as the Flatté model [98] since its mass is close to the $K\bar{K}$ threshold. The constants $g_{\pi\pi}$ and g_{KK} are the $f_0(980)$ couplings to $\pi^+\pi^-$ and K^+K^- final states, respectively. The $\rho_{\pi\pi(KK)}$ factors are given by the Lorentz-invariant phase space

$$\begin{aligned}\rho_{\pi\pi} &= \frac{2}{3}\sqrt{1 - \frac{4m_{\pi^\pm}^2}{\omega^2}} + \frac{1}{3}\sqrt{1 - \frac{4m_{\pi^0}^2}{\omega^2}}, \\ \rho_{KK} &= \frac{1}{2}\sqrt{1 - \frac{4m_{K^\pm}^2}{\omega^2}} + \frac{1}{2}\sqrt{1 - \frac{4m_{K^0}^2}{\omega^2}}.\end{aligned}\quad (18)$$

For the non-strange case, only the resonance $f_0(500)$ is including here, which can be modeled using two alternative approaches, the BW function [58] and the Bugg [99] formalisms. The BW model read as

$$F_{\pi\pi}^{d\bar{d}}(\omega) = \frac{c_{BW}m_{f_0(500)}^2}{m_{f_0(500)}^2 - \omega^2 - im_{f_0(500)}\Gamma_{f_0(500)}(\omega^2)},\quad (19)$$

with $c_{BW} = 3.5$ [58]. The Bugg resonant line shape [99], with more theoretically motivated shape parameters, has been used by several recent analyses, e.g. Refs. [95, 96, 100, 101],

$$F_{\pi\pi}^{d\bar{d}}(\omega) = c_{Bugg}m_r\Gamma_1(\omega^2)[m_r^2 - \omega^2 - g_1^2\frac{\omega^2 - s_A}{m_r^2 - s_A}z(\omega^2) - im_r\sum_{i=1}^4\Gamma_i(\omega^2)]^{-1},\quad (20)$$

with c_{Bugg} being a tunable parameter. Its value is set to 1.6 so that the corresponding PQCD prediction of $\mathcal{B}(\bar{B}^0 \rightarrow J/\psi f_0(500)(\rightarrow \pi^+\pi^-)) = 8.5 \times 10^{-6}$ is consistent with the LHCb data $(8.8 \pm 0.5^{+1.1}_{-1.5}) \times 10^{-6}$ in Ref. [102]. Variables and parameters in above equation are not shown here for readability, which can be found in [99]. We also note that the $f_0(500)$ can be represented as a simple pole [103–106], parametrized as

$$A_\sigma(\omega) = \frac{1}{\omega^2 - s_\sigma},\quad (21)$$

where s_σ is the square of the pole position $\sqrt{s_\sigma} = m_\sigma - i\Gamma_\sigma$, extracted from the data. However, Eq. (21) carries a dimension and is not normalized to the unity as $\omega \rightarrow 0$. Thus it is not appropriate to be taken as a form factor in the PQCD approach in current form. The exact form factor corresponding to the pole model in PQCD should be taken into account in the future.

For the scalar form factor of $K\pi$ system, we employ the LASS line shape [107], which consists of the $K_0^*(1430)$ resonance as well as an effective-range nonresonant component,

$$\begin{aligned}F_{K\pi}(\omega) &= \frac{\omega}{|\vec{p}_1|} \cdot \frac{1}{\cot \delta_B - i} + e^{2i\delta_B} \frac{m_0^2\Gamma_0/|\vec{p}_0|}{m_0^2 - \omega^2 - im_0^2\frac{\Gamma_0}{\omega} \frac{|\vec{p}_1|}{|\vec{p}_0|}}, \\ \cot \delta_B &= \frac{1}{a|\vec{p}_1|} + \frac{1}{2}b|\vec{p}_1|.\end{aligned}\quad (22)$$

m_0 and Γ_0 are the pole mass and width of the $K^*(1430)$, while scattering length a and b effective range are parameters that describe the shape, whose numbers are taken from measurements at the LASS experiment and tabulated in next section. \vec{p}_0 is the value of \vec{p}_1 calculated using the nominal resonance mass, m_0 . The phase factor δ_B is needed for the conservation of unitarity. It is worth noting that the LASS parameterization has a range of applicability up to about the charm hadron mass [108, 109] in the $K\pi$ invariant mass, which is just approaching the upper bound of $M - m$ for the charmonium B decays. Therefore, it is not necessary to introduce a nonphysical cutoff here and the LASS model is appropriate to describe the $K\pi$ S -wave in the decays under study.

As for the case of $K\bar{K}$ system, we follow Ref. [62] to take the form as,

$$\begin{aligned}F_{KK}(\omega) &= \left[\frac{m_{f_0(980)}^2}{m_{f_0(980)}^2 - \omega^2 - im_{f_0(980)}(g_{\pi\pi}\rho_{\pi\pi} + g_{KK}\rho_{KK}F_{KK}^2)} \right. \\ &\quad \left. + \frac{c_{f_0(1370)}m_{f_0(1370)}^2}{m_{f_0(1370)}^2 - \omega^2 - im_{f_0(1370)}\Gamma_{f_0(1370)}(\omega^2)} \right] (1 + c_{f_0(1370)})^{-1}.\end{aligned}\quad (23)$$

with $c_{f_0(1370)} = 0.12e^{-i\pi/2}$ [62], which yields the branching ratios of the $f_0(980)$ and $f_0(1370)$ components in $B_s \rightarrow J/\psi K^+ K^-$ are consistent with the data, simultaneously. The exponential term $F_{KK} = e^{-\alpha q_k^2}$ is introduced above the KK threshold to reduce the ρ_{KK} factor as ω increases, where q_k is momentum of kaon in the KK rest frame and $\alpha = 2.0 \pm 0.25 \text{ GeV}^{-2}$ [94, 110].

Now we will present the formulas of amplitude for the quasi-two-body decay mediated by scalar resonances. Performing the calculations to the factorizable and nonfactorizable diagrams in Fig. 1, one gets the following expressions:

$$\begin{aligned} \mathcal{F}^{LL} = & -8\pi C_F f_{\chi_{c1}} M^3 \int_0^1 dx_B dz \int_0^\infty db_B db_B b db \phi_B(x_B, b_B) \\ & \{ [\omega \phi_S^s (-2f^+ g^+ z - g^- + g^+) + \omega \phi_S^t (-2f^+ g^+ z + g^- + g^+) + M \phi_S^0 (f^+ g^+ (f^+ z + 1) - f^- g^-)] \\ & \alpha_s(t_a) e^{-S_{ab}(t_a)} h(\alpha_e, \beta_a, b_B, b_1) S_t(x_3) + [M \phi_S^0 ((f^- + 1) f^+ g^+ - g^- (f^- + f^+ (f^- - x_B))) - 2\omega \phi_S^s \\ & (g^- (-f^- + x_B - 1) + (f^+ + 1) g^+)] \alpha_s(t_b) e^{-S_{ab}(t_b)} h(\alpha_e, \beta_b, b_1, b_B) S_t(x_B) \}, \end{aligned} \quad (24)$$

$$\begin{aligned} \mathcal{M}^{LL} = & 16\sqrt{2}\pi C_F M^3 \int_0^1 dx_B dz dx_3 \int_0^\infty db_B db_B b_3 db_3 \phi_B(x_B, b_B) \\ & [M r_{\chi_L}(x_3) \phi_S^0 (2f^+ (g^+)^2 x_3 + g^- (f^+ x_B + f^- (-2f^+ z - 2g^- x_3 + x_B)) + f^+ g^+ ((f^- + f^+) z - 2x_B)) \\ & - 2r_{\chi_L}(x_3) \omega \phi_S^s (f^+ g^+ z + g^- x_B) + 4g^- g^+ r_{c\chi_t}(x_3) \omega \phi_S^t \alpha_s(t_d) e^{-S_{cd}(t_d)} h(\beta_d, \alpha_e, b, b_B), \end{aligned} \quad (25)$$

$$\mathcal{F}^{LR} = -\mathcal{F}^{LL}, \quad \mathcal{M}^{SP} = \mathcal{M}^{LL}, \quad (26)$$

with $r_c = m_c/M$ and m_c is the charm quark mass; $C_f = 4/3$ is a color factor. The superscript LL , LR , and SP refers to the contributions from $(V-A) \otimes (V-A)$, $(V-A) \otimes (V+A)$ and $(S-P) \otimes (S+P)$ operators, respectively. The hard functions h and the threshold resummation factor $S_t(x)$ are adopted from Ref. [111]. α and β_i with $i = a, b, d$ denote the virtuality of the internal gluon and quark, respectively, expressed as

$$\begin{aligned} \alpha &= z x_B f^+ M^2, \\ \beta_a &= z f^+ M^2, \\ \beta_b &= -f^+ (f^- - x_B) M^2, \\ \beta_d &= -(f^+ z + g^- x_3)(g^+ x_3 - x_B) M^2 + m_c^2. \end{aligned} \quad (27)$$

The hard scale t_i is chosen as the largest scale of the virtualities of the internal particles in the hard amplitudes:

$$\begin{aligned} t_a &= \max(\sqrt{\alpha}, \sqrt{\beta_a}, 1/b, 1/b_B), \\ t_b &= \max(\sqrt{\alpha}, \sqrt{\beta_b}, 1/b, 1/b_B), \\ t_d &= \max(\sqrt{\alpha}, \sqrt{\beta_d}, 1/b_3, 1/b_B). \end{aligned} \quad (28)$$

The Sudakov exponents are given by

$$\begin{aligned} S_{ab}(t) &= s\left(\frac{M}{\sqrt{2}} x_B, b_B\right) + s\left(\frac{M}{\sqrt{2}} f^+ z, b\right) + s\left(\frac{M}{\sqrt{2}} f^+ (1-z), b\right) + \frac{5}{3} \int_{1/b_B}^t \frac{d\mu}{\mu} \gamma_q(\mu) + 2 \int_{1/b}^t \frac{d\mu}{\mu} \gamma_q(\mu), \\ S_{cd}(t) &= s\left(\frac{M}{\sqrt{2}} x_B, b_B\right) + s\left(\frac{M}{\sqrt{2}} f^+ z, b_B\right) + s\left(\frac{M}{\sqrt{2}} f^+ (1-z), b_B\right) + s\left(\frac{M}{\sqrt{2}} g^+ x_3, b_3\right) + s\left(\frac{M}{\sqrt{2}} g^+ (1-x_3), b_3\right) \\ &+ \frac{11}{3} \int_{1/b_B}^t \frac{d\mu}{\mu} \gamma_q(\mu) + 2 \int_{1/b_3}^t \frac{d\mu}{\mu} \gamma_q(\mu), \end{aligned} \quad (29)$$

where $\gamma_q = -\alpha_s/\pi$ is the quark anomalous dimension, and the explicit expression of the function $s(Q, b)$ can be found in [112].

By combining the contributions from different diagrams with the corresponding Wilson coefficients, the full decay amplitude can be recast to

$$\begin{aligned} \mathcal{A} = & \frac{G_F}{\sqrt{2}} \left\{ \lambda_c \left[a_2 \mathcal{F}^{LL} + C_2 \mathcal{M}^{LL} \right] - \lambda_t \left[(a_3 + a_9) \mathcal{F}^{LL} + \right. \right. \\ & \left. \left. (a_5 + a_7) \mathcal{F}^{LR} + (C_4 + C_{10}) \mathcal{M}^{LL} + (C_6 + C_8) \mathcal{M}^{SP} \right] \right\}, \end{aligned} \quad (30)$$

TABLE I: A summary of the relevant resonance parameters.

Resonance	Model	Parameters
$f_0(500)$	BW	$m_R = 0.50\text{GeV}, \Gamma_R = 0.40\text{GeV}$ [58]
	Bugg	See Ref. [99]
$f_0(980)$	Flatté	$m_R = 0.99\text{ GeV}[1], g_{\pi\pi} = 0.167\text{GeV}, g_{KK}/g_{\pi\pi} = 3.47[102]$
$f_0(1370)$	BW	$m_R = 1.475\text{GeV}, \Gamma_R = 0.113\text{GeV}[94]$
$f_0(1500)$	BW	$m_R = 1.50\text{GeV}, \Gamma_R = 0.12\text{GeV}[94]$
$f_0(1790)$	BW	$m_R = 1.81\text{GeV}, \Gamma_R = 0.32\text{GeV}$ [58]
$(K\pi)_{S\text{-wave}}$	LASS	$m_R = 1.435\text{GeV}, \Gamma_R = 0.279\text{GeV}, a = 1.94\text{GeV}^{-1}, b = 1.76\text{GeV}^{-1}[116]$

with

$$a_2 = C_1 + \frac{1}{3}C_2, a_3 = C_3 + \frac{1}{3}C_4, a_9 = C_9 + \frac{1}{3}C_{10}, a_5 = C_5 + \frac{1}{3}C_6, a_7 = C_7 + \frac{1}{3}C_8. \quad (31)$$

The quantities $\lambda_p \equiv V_{pb}^* V_{pq}$ with $p = c, t$ and $q = d, s$ encode the CKM factors. We also consider the vertex corrections, whose effects can be combined into the coefficients a_i in Eq. (31) as [113–115]

$$\begin{aligned} a_2 &\rightarrow a_2 + \frac{\alpha_s C_f}{4\pi N_c} C_2 \left[-18 - 12\ln\left(\frac{t}{m_b}\right) + f_I \right], \\ a_3 + a_9 &\rightarrow a_3 + a_9 + \frac{\alpha_s C_f}{4\pi N_c} (C_4 + C_{10}) \left[-18 - 12\ln\left(\frac{t}{m_b}\right) + f_I \right], \\ a_5 + a_7 &\rightarrow a_5 + a_7 - \frac{\alpha_s C_f}{4\pi N_c} (C_6 + C_8) \left[-6 - 12\ln\left(\frac{t}{m_b}\right) + f_I \right], \end{aligned} \quad (32)$$

where the detail calculations for f_I refer to Refs. [49, 52].

Finally, the differential branching ratio for the $B \rightarrow \chi_{c1} hh'$ process reads as

$$\frac{d\mathcal{B}}{d\omega} = \frac{\tau\omega|\vec{p}_1||\vec{p}_3|}{32\pi^3 M^3} |\mathcal{A}|^2. \quad (33)$$

III. RESULTS AND DISCUSSIONS

This section serves to summarize all parameter values required for numerical calculations. The meson and heavy quark masses (GeV), lifetimes (ps), and the Wolfenstein parameters are taken from Particle Data Group [1],

$$\begin{aligned} M_{B_s} &= 5.37, \quad M_B = 5.28, \quad m_K = 0.494, \quad m_\pi = 0.14, \\ m_{\chi_{c1}(1P)} &= 3.51067, \quad m_{\chi_{c1}(2P)} = 3.87169, \quad m_b = 4.8, \quad \bar{m}_c(\bar{m}_c) = 1.275, \\ \tau_{B^+} &= 1.638, \quad \tau_{B_s} = 1.51, \quad \tau_{B^0} = 1.51, \\ \lambda &= 0.22650, \quad A = 0.790, \quad \bar{\rho} = 0.141, \quad \bar{\eta} = 0.357. \end{aligned} \quad (34)$$

The B decay constants are set to the values $f_B = 0.19\text{ GeV}$ and $f_{B_s} = 0.24\text{ GeV}$ [66]. Since there is no measurement for $f_{\chi_{c1}(2P)}$, we assume $f_{\chi_{c1}(2P)}^{(\perp)} = f_{\chi_{c1}(1P)}^{(\perp)} = 0.335\text{ GeV}$ [50, 51, 53] and do not distinguish the vector and tensor decay constants in subsequent calculations. The relevant resonance parameters are listed in Table I. Other parameters appearing in the two meson DAs have been specified before.

Using above parameters, we calculate the CP average branching ratios of various S -wave components for the neutral B^0 and B_s^0 decays by integrating the differential branching ratio in Eq. (33) with respect to ω . The corresponding numbers for the charge analogous B^+ decay processes can be obtained by multiplying the B^0 ones with a factor of τ_{B^+}/τ_{B^0} in the limit of isospin symmetry. The theoretical errors correspond to the uncertainties due to the shape parameters $\omega_{B_{(s)}} = 0.40 \pm 0.04(0.48 \pm 0.05)\text{ GeV}$ for the $B_{(s)}$ meson wave function, the hard scales t defined in Eq. (28), that vary from $0.75t$ to $1.25t$, and the Gegenbauer moments $a_{\pi\pi} = 0.2 \pm 0.2$ [58], $a_{KK} = 0.80 \pm 0.16$ [62], $B_1 = -0.57 \pm 0.13$ and $B_3 = -0.42 \pm 0.22$ [88, 89] associated with the twist-2 DAs as shown in Eq. (15), respectively. It is necessary to stress that the twist-3 DAs of the meson pair in this work are taken as the asymptotic forms for lack of better results from nonperturbative methods, which may give significant uncertainties. In the following, we will discuss the relevant numerical results in turn.

TABLE II: Branching ratios of S -wave resonant contributions to the $B_s^0 \rightarrow \chi_{c1}(1P, 2P)\pi^+\pi^-$ decays. The theoretical errors correspond to the uncertainties due to the shape parameters ω_{B_s} , the hard scale t , and the Gegenbauer moment $a_{\pi\pi}$, respectively.

Modes	$\mathcal{B}(R = f_0(980))$	$\mathcal{B}(R = f_0(1500))$	$\mathcal{B}(R = f_0(1790))$	$\mathcal{B}(S\text{-wave})$
$B_s^0 \rightarrow \chi_{c1}(1P)\pi^+\pi^-$	$(7.6^{+3.4+0.5+0.9}_{-2.0-0.5-0.6}) \times 10^{-5}$	$(7.8^{+0.7+0.6+0.2}_{-0.9-0.4-0.3}) \times 10^{-6}$	$(6.4^{+1.5+0.0+0.5}_{-1.2-0.2-0.5}) \times 10^{-7}$	$(1.1^{+0.3+0.0+0.1}_{-0.3-0.1-0.1}) \times 10^{-4}$
$B_s^0 \rightarrow \chi_{c1}(2P)\pi^+\pi^-$	$(7.1^{+2.4+0.2+0.6}_{-1.8-0.5-0.4}) \times 10^{-5}$	$(1.8^{+0.5+0.0+0.2}_{-0.3-0.0-0.1}) \times 10^{-6}$	$(1.9^{+0.5+0.1+0.1}_{-0.3-0.1-0.1}) \times 10^{-7}$	$(8.6^{+2.4+0.2+0.6}_{-2.1-0.7-0.5}) \times 10^{-5}$

A. $B_s^0 \rightarrow \chi_{c1}\pi^+\pi^-$

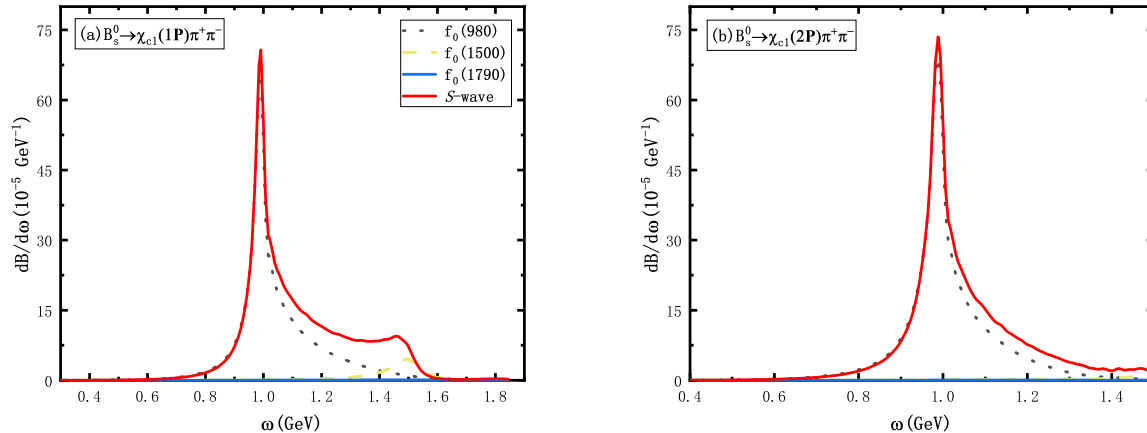


FIG. 2: The ω dependence of the differential decay branching ratios $dB/d\omega$ for the decay modes (a) $B_s^0 \rightarrow \chi_{c1}(1P)\pi^+\pi^-$ and (b) $B_s^0 \rightarrow \chi_{c1}(2P)\pi^+\pi^-$. The contributions from $f_0(980)$, $f_0(1500)$ and $f_0(1790)$ components are shown by the dotted gray, dashed khaki and solid blue curves, respectively, while the solid red curves represent the total S -wave contributions.

As mentioned in the previous section, three resonances were considered in the $B_s^0 \rightarrow \chi_{c1}\pi^+\pi^-$ decay, namely, $f_0(980)$, $f_0(1500)$, and $f_0(1790)$. The calculated branching ratios of concerned resonances are collected in Table II. The last column corresponds to the total S -wave branching ratios. It is evident that the largest contribution comes from the $f_0(980)$ component, which accounts for 69%(83%) of the $\chi_{c1}(1P(2P))$ mode. The contributions from high resonances suffer seriously suppression since the pole masses are approaching the upper bound of the two pion invariant mass spectra. In particular, the nominal mass of $f_0(1790)$ falls outside the kinematically allowed mass range for the $\chi_{c1}(2P)$ mode and the residual contribution in the tail region of the BW function, also known as virtual contribution, is expected to be fairly small. The corresponding branching ratio is predicted to be of order 10^{-7} , much smaller than that of $B_s \rightarrow \chi_{c1}f_0(1790)(\rightarrow \pi^+\pi^-)$. The total S -wave branching ratios for the two channels can reach the 10^{-4} level, to be compared with those of in J/ψ modes [58, 97], which is large enough to permit a measurement.

In Fig 2, we track the differential branching ratios for various resonances as a function of the $\pi^+\pi^-$ invariant mass, which we vary from $2m_\pi$ up to $M - m$. The dotted gray, dashed khaki and solid blue curves correspond to the $f_0(980)$, $f_0(1500)$, and $f_0(1790)$ resonances, respectively, while the solid red curves represent the total S -wave contributions. Note that the mass difference between $\chi_{c1}(1P)$ and $\chi_{c1}(2P)$ causes significant differences in the range spanned in the respective decay modes. One can see a clear signal from the $f_0(980)$ resonance, accompanied by $f_0(1500)$, while the amount of $f_0(1790)$ are less than 1% of the total S -wave contributions. A dip in Fig. 2(a) in the invariant mass region of 1.2-1.4 GeV is ascribed to the interference between the $f_0(980)$ and $f_0(1500)$ channels. However, such dip is not observed in Fig. 2(b) because the $f_0(1500)$ component suffer strongly phase space suppression for the $\chi_{c1}(2P)$ mode.

TABLE III: Branching ratios of S -wave resonant contributions to the $B^0 \rightarrow \chi_{c1}(1P, 2P)f_0(500)(\rightarrow \pi\pi)$ decays. The theoretical errors correspond to the uncertainties due to the shape parameters ω_B , the hard scale t , and the Gegenbauer moment $a_{\pi\pi}$, respectively.

Modes	$\mathcal{B}(\text{BW})$	$\mathcal{B}(\text{Bugg})$	$\mathcal{B}(\text{pole})$
$B^0 \rightarrow \chi_{c1}(1P)f_0(500)(\rightarrow \pi^+\pi^-)$	$(2.9_{-0.7-0.1-0.5}^{+1.0+0.1+1.1}) \times 10^{-6}$	$(2.8_{-0.6-0.0-0.3}^{+0.6+0.0+0.4}) \times 10^{-6}$	$(4.9_{-1.2-0.2-0.7}^{+1.5+0.1+1.2}) \times 10^{-6}$
$B^0 \rightarrow \chi_{c1}(2P)f_0(500)(\rightarrow \pi^+\pi^-)$	$(2.8_{-0.7-0.1-0.0}^{+0.9+0.0+0.5}) \times 10^{-6}$	$(1.7_{-0.3-0.0-0.0}^{+0.4+0.0+0.1}) \times 10^{-6}$	$(4.3_{-1.0-0.1-0.0}^{+1.2+0.0+0.6}) \times 10^{-6}$

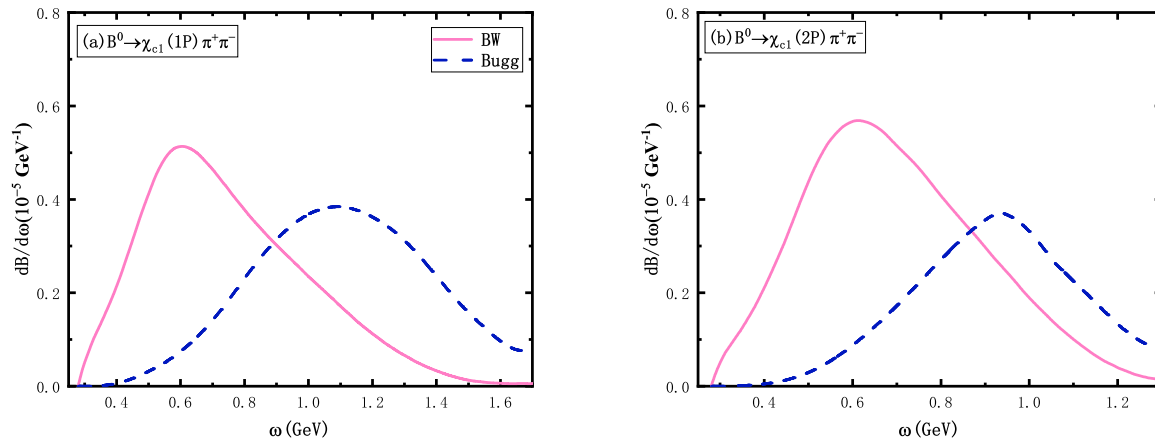


FIG. 3: (a) $\text{dB}/\text{d}\omega$ invariant-mass distribution for the $B^0 \rightarrow \chi_{c1}(1P)f_0(500)(\rightarrow \pi^+\pi^-)$ decay with two different descriptions for the $f_0(500)$ resonance. Similar curves shown in (b) but for $B^0 \rightarrow \chi_{c1}(2P)f_0(500)(\rightarrow \pi^+\pi^-)$ mode. The BW and Bugg models are shown by the solid pink and dashed blue lines, respectively.

B. $B^0 \rightarrow \chi_{c1}\pi^+\pi^-$

The branching ratios of $B^0 \rightarrow \chi_{c1}(1P, 2P)f_0(500)(\rightarrow \pi^+\pi^-)$ decays, calculated for both BW and Bugg models, are presented for comparison in Table III. The dependence of differential branching ratios as a function of the invariant mass are also shown in Fig. 3 for the aforementioned two line shapes, where the solid pink and dashed blue lines correspond to the BW and Bugg models, respectively. The two curves have a broad bump with different behaviors in shape. In the BW model, the peak at the resonance is usually highly dominating and the majority of the resonant contribution focus naturally on the mass range of $f_0(500)$. Although $f_0(500)$ is very broad, the predominated mass region still far away from the the upper bound of allowed phase space, $M - m$. However, the strength of Bugg model is slightly small, as seen in Fig.3, the spectrum bump is located above the pole mass of $f_0(500)$ because the substantial coupling of $f_0(500)$ to KK and $\eta\eta$ are included. As a consequence, the contribution from the high-mass regions can not be ignored. From Table III, we find $\mathcal{B}(B^0 \rightarrow \chi_{c1}(1P)f_0(500)(\rightarrow \pi^+\pi^-))$ and $\mathcal{B}(B^0 \rightarrow \chi_{c1}(2P)f_0(500)(\rightarrow \pi^+\pi^-))$ are of comparable size for the BW model, but the latter is relatively small owing to the phase space suppression for the Bugg one.

C. $B_{(s)}^0 \rightarrow \chi_{c1}K\pi$

Since the LASS description for the $K\pi$ S -wave contained both resonant and nonresonant components as shown in Eq. (22). We summarize the branching ratios of $K^*(1430)$ resonant and nonresonant component as well as the total S -wave contribution in Table IV separately. The invariant mass dependence of the differential decay rates for the two components are shown in Fig. 4. Analogous to the pattern of the $B_{(s)} \rightarrow J/\psi K\pi$ decays in our previous analysis [59], the contributions from the resonant and nonresonant components in this work are comparable in size. Hence, the nonresonant contributions also play an essential role in $B_{(s)} \rightarrow \chi_{c1}K\pi$ decays. The constructive interference between the resonant and nonresonant contributions lead to large S -wave branching ratios as shown in Fig. 4, especially the

TABLE IV: Branching ratios of various S -wave components to the $B_{(s)} \rightarrow \chi_{c1}(1P, 2P)K\pi$ decays. The theoretical errors correspond to the uncertainties due to the shape parameters $\omega_{B_{(s)}}$, the hard scale t , and the Gegenbauer moments $B_{1,3}$, respectively.

Modes	$\mathcal{B}(R = K_0^*(1430))$	$\mathcal{B}(\text{LASS NR})$	$\mathcal{B}(S\text{-wave})$
$B_s^0 \rightarrow \chi_{c1}(1P)K^- \pi^+$	$(3.8^{+0.7+0.3+0.5}_{-0.6-0.2-0.4}) \times 10^{-6}$	$(3.4^{+0.9+0.3+0.4}_{-0.7-0.2-0.4}) \times 10^{-6}$	$(6.9^{+1.9+0.5+0.9}_{-1.6-0.5-0.8}) \times 10^{-6}$
$B_s^0 \rightarrow \chi_{c1}(2P)K^- \pi^+$	$(1.5^{+0.2+0.0+0.1}_{-0.3-0.1-0.2}) \times 10^{-6}$	$(1.8^{+0.6+0.1+0.4}_{-0.3-0.1-0.1}) \times 10^{-6}$	$(4.4^{+1.2+0.2+0.6}_{-0.9-0.3-0.5}) \times 10^{-6}$
$B^0 \rightarrow \chi_{c1}(1P)K^+ \pi^-$	$(5.1^{+0.3+0.1+0.5}_{-0.6-0.2-0.6}) \times 10^{-5}$	$(5.3^{+1.0+0.1+0.5}_{-1.0-0.2-0.5}) \times 10^{-5}$	$(1.1^{+0.2+0.1+0.2}_{-0.2-0.0-0.1}) \times 10^{-4}$
$B^0 \rightarrow \chi_{c1}(2P)K^+ \pi^-$	$(1.6^{+0.2+0.0+0.1}_{-0.3-0.1-0.2}) \times 10^{-5}$	$(2.8^{+0.5+0.0+0.4}_{-0.6-0.1-0.4}) \times 10^{-5}$	$(6.4^{+1.2+0.0+0.7}_{-1.2-0.1-0.7}) \times 10^{-5}$

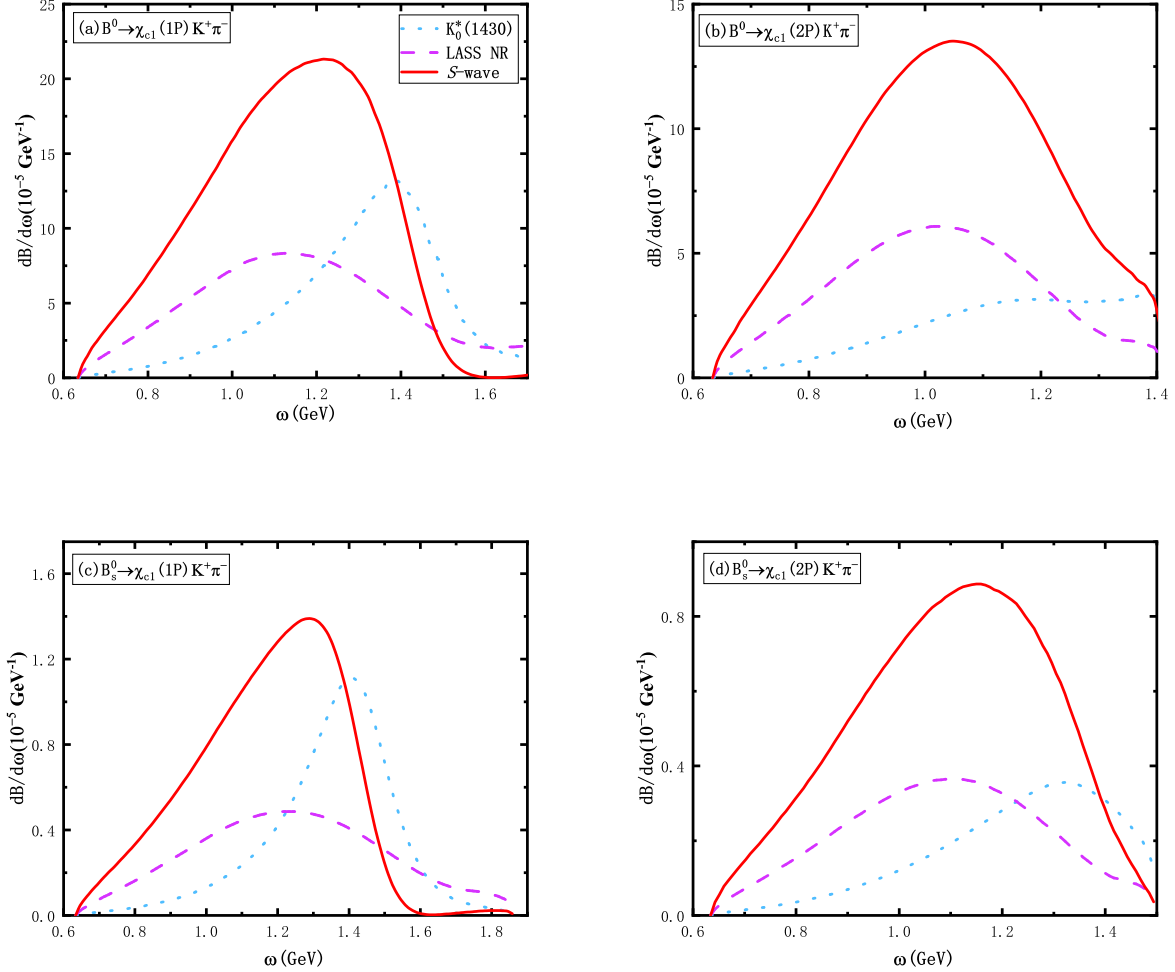


FIG. 4: S -wave contributions to the differential branching ratios of the modes (a) $B^0 \rightarrow \chi_{c1}(1P)K^+\pi^-$, (b) $B^0 \rightarrow \chi_{c1}(2P)K^+\pi^-$, (c) $B_s^0 \rightarrow \chi_{c1}(1P)K^+\pi^-$, and (d) $B_s^0 \rightarrow \chi_{c1}(2P)K^+\pi^-$. The dotted blue, dashed violet, and solid red show the contributions from resonances $K_0^*(1430)$, LASS NR and their combinatorial, respectively.

$B^0 \rightarrow \chi_{c1}(1P)K^+\pi^-$ mode has a large branching ratio of order 10^{-4} . The corresponding B_s channels have relatively small branching ratios (10^{-6}) comparing with the B^0 modes due to the CKM suppression $|V_{cd}/V_{cs}| \sim \lambda$.

From the fit fraction of the $K_0^*(1430)$ component in $\bar{B}^0 \rightarrow \chi_{c1}K^-\pi^+$ decay analyzed in the isobar model [7] and

TABLE V: Branching ratios of S -wave resonant contributions to the $B_s^0 \rightarrow \chi_{c1}(1P, 2P)K^+K^-$ decays. The theoretical errors correspond to the uncertainties due to the shape parameter ω_{B_s} , the hard scale t , and the Gegenbauer moment a_{KK} , respectively.

Modes	$\mathcal{B}(R = f_0(980))$	$\mathcal{B}(R = f_0(1370))$	$\mathcal{B}(S\text{-wave})$
$B_s^0 \rightarrow \chi_{c1}(1P)K^+K^-$	$(3.5^{+1.1+0.5+0.3}_{-0.8-0.3-0.2}) \times 10^{-5}$	$(9.2^{+0.7+0.8+0.3}_{-1.1-0.7-0.3}) \times 10^{-6}$	$(3.9^{+1.0+0.5+0.2}_{-0.8-0.3-0.2}) \times 10^{-5}$
$B_s^0 \rightarrow \chi_{c1}(2P)K^+K^-$	$(2.7^{+0.7+0.2+0.2}_{-0.6-0.3-0.2}) \times 10^{-5}$	$(2.4^{+0.5+0.0+0.1}_{-0.5-0.2-0.2}) \times 10^{-6}$	$(2.4^{+0.7+0.2+0.2}_{-0.6-0.2-0.2}) \times 10^{-5}$

the three-body branching ratio $\mathcal{B}(\bar{B}^0 \rightarrow \chi_{c1}K^-\pi^+) = (3.83 \pm 0.10 \pm 0.39) \times 10^{-4}$ measured by Belle [7], we obtain

$$\mathcal{B}(B^0 \rightarrow \chi_{c1}K_0^*(1430)(\rightarrow K^+\pi^-))_{\text{expt}} = \begin{cases} (8.6 \pm 2.4) \times 10^{-5} & \text{S1,} \\ (7.1 \pm 2.1) \times 10^{-5} & \text{S2,} \end{cases}$$

where S1 and S2 denote the two solutions from single- and double- Z^+ resonance scenarios in the $\chi_{c1}\pi^+$ invariant mass distribution, respectively. One can see from Table IV that the predicted branching ratio $\mathcal{B}(\bar{B}^0 \rightarrow \chi_{c1}K_0^*(1430)(\rightarrow K^-\pi^+)) = (5.1^{+0.6}_{-0.8}) \times 10^{-5}$ is compatible with above two solutions within errors.

The BABAR collaboration measured the three-body branching ratio, $\mathcal{B}(\bar{B}^0 \rightarrow \chi_{c1}K^-\pi^+) = (5.11 \pm 0.14 \pm 0.28) \times 10^{-4}$ [117]. Meanwhile, the S , P , and D -wave fractions are fitted from the analysis of the $K\pi$ mass spectra. It is found that the S -wave fraction in $\bar{B}^0 \rightarrow \chi_{c1}K^-\pi^+$ are larger than the corresponding J/ψ and $\psi(2S)$ modes. With the measured S -wave fractions of $f_S = (40.4 \pm 2.2)\%$, the corresponding S -wave branching fractions, calculated as

$$\mathcal{B}(\bar{B}^0 \rightarrow \chi_{c1}(K^-\pi^+)_S) = \mathcal{B}(\bar{B}^0 \rightarrow \chi_{c1}K^-\pi^+) \times f_S = 2.1^{+0.1}_{-0.2} \times 10^{-4}, \quad (35)$$

which is twice than our prediction in Table IV. We note that the three-body branching ratio measured by BABAR is typically larger than the previous measurement by Belle [7] and also larger than the updated measurement of $\mathcal{B}(\bar{B}^0 \rightarrow \chi_{c1}K^-\pi^+) = (4.97 \pm 0.12 \pm 0.28) \times 10^{-4}$ in [9]. As an aside, the quoted uncertainty for the fitted S -wave fraction is statistical only, thereby improving precision on both the theoretical and experimental values would be highly desirable.

D. $B_s^0 \rightarrow \chi_{c1}K^+K^-$

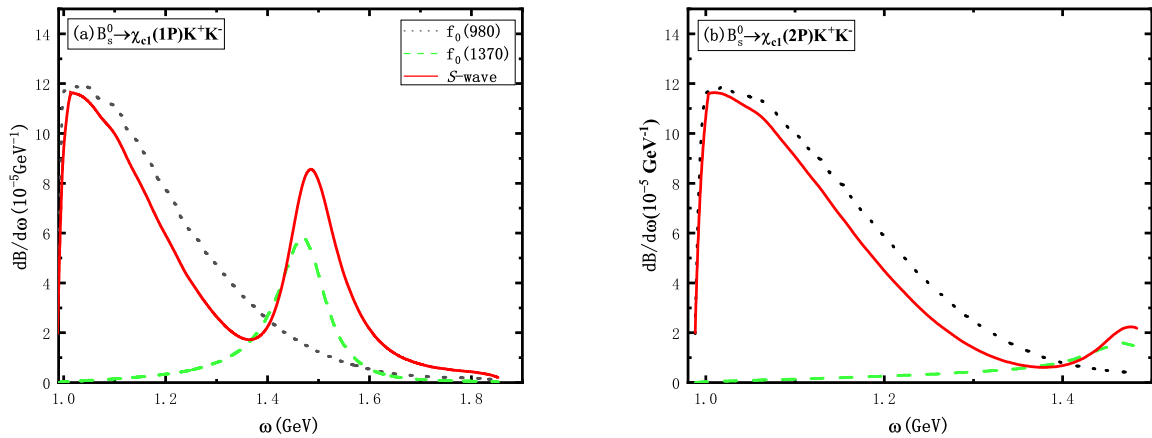


FIG. 5: Various resonance contributions to the differential branching ratios of the modes (a) $B_s^0 \rightarrow \chi_{c1}(1P)K^+K^-$ and (b) $B_s^0 \rightarrow \chi_{c1}(2P)K^+K^-$. The dotted gray, dashed green and solid red curves show the resonances $f_0(980)$, $f_0(1370)$, and their combinatorial contributions, respectively.

We next turn to the $B_s^0 \rightarrow \chi_{c1} K^+ K^-$ decay which receives two resonant contributions from $f_0(980)$ and $f_0(1370)$ in the $K^+ K^-$ invariant mass spectrum. The predicted branching ratios are depicted in Table V, while the corresponding differential distributions over ω are plotted in Fig. 5. The red (solid) curves denote the total contribution, while individual terms are given by the gray (dotted) lines for $f_0(980)$ and green (dashed) lines for $f_0(1370)$. It is clear that the S -wave contributions are dominated by $f_0(980)$, while the $f_0(1370)$ component are several times smaller. The total S -wave branching ratios reach the order of 10^{-5} , which are comparable with those of $\pi\pi$ modes in Table II. Since $f_0(980)$ can decay into a kaon or a pion pair, we can estimate the relative branching ratios

$$\mathcal{R} = \frac{\mathcal{B}(B_s^0 \rightarrow \chi_{c1} f_0(980) (\rightarrow K^+ K^-))}{\mathcal{B}(B_s^0 \rightarrow \chi_{c1} f_0(980) (\rightarrow \pi^+ \pi^-))}. \quad (36)$$

Combining Tables II and V, the ratio \mathcal{R} is predicted to be $0.46_{-0.19}^{+0.24} (0.37_{-0.14}^{+0.18})$ for the $1P(2P)$ state mode, which is comparable with our previous prediction for that of J/ψ with $\mathcal{R}(J/\psi) = 0.37_{-0.13}^{+0.23}$ [62]. In the narrow-width limit, Eq.(36) simplifies to

$$\mathcal{R} \approx \frac{\mathcal{B}(f_0(980) \rightarrow K^+ K^-)}{\mathcal{B}(f_0(980) \rightarrow \pi^+ \pi^-)}, \quad (37)$$

where the common term $\mathcal{B}(B_s^0 \rightarrow \chi_{c1} f_0(980))$ in the numerator and denominator cancel out. The weighted average of \mathcal{R} from BABAR [118] and BES [119] measurements yields $\mathcal{R}_{\text{expt}} = 0.35_{-0.14}^{+0.15}$ [102]. Our estimates turns out to be consistent with this average value.

From Tables II,III,IV, and V, one can see that the branching ratios of the lower mass resonances between $\chi_{c1}(1P)$ and $\chi_{c1}(2P)$ modes are comparable, whereas in the case of the higher mass resonances, the corresponding branching ratios for the latter are typically smaller due to the phase space suppression. Since the $\chi_{c1}(2P)$ modes are received less theoretical and experimental attention, we wait for future comparison, which may help us to further clarify the structure of $X(3872)$.

IV. CONCLUSION

We have analyzed the three-body decays $B_{(s)} \rightarrow \chi_{c1} h h'$ in the $h h'$ invariant mass spectrum with S -wave configuration in the perturbative QCD approach. The final-state pseudoscalar meson $h^{(\prime)}$ is restricted to be a kaon or a pion. The S -wave contributions are parametrized into the timelike form factors involved in the two meson DAs, which have been well established in the corresponding J/ψ decays.

The strange scalar form factor for the $\pi\pi$ pair is described by the coherent sum of three scalar resonances $f_0(980)$, $f_0(1500)$, and $f_0(1790)$. Except for $f_0(980)$, parametrized by a Flatté line shape, the latter two resonances are modeled by the Breit-Wigner function. The non-strange scalar form factor contains only the $f_0(500)$ resonance, which are modeled with two alternative shapes, the BW and Bugg formalisms. Although the resultant invariant mass distributions for the two models show a different behavior, the integrated branching ratios over the entire phase space are comparable. The $K\pi$ timelike form factor is described by the conventional LASS parametrization, which consists $K^*(1430)$ resonance together with an effective range nonresonant component. It is found that the contributions from the two pieces are of comparable size. In the KK sector, the corresponding timelike form factor is parametrized by a linear combination of the $f_0(980)$ and $f_0(1370)$ resonances, where the latter is also modeled by the BW line shape.

By using the well established two-meson DAs, we have calculated the branching ratios together with the differential distributions of various components in the processes under consideration. The branching ratio of $B \rightarrow \chi_{c1} K_0^*(1430) (\rightarrow K^+ \pi^-)$ is predicted to be $(5.1_{-0.8}^{+0.6}) \times 10^{-5}$, which is in agreement with the Belle measurement, while the obtained S -wave branching ratio is smaller than the BaBar data by a factor of 2. The branching ratios for some Cabibbo-favored decays are large of order 10^{-4} , whereas those of the Cabibbo-suppressed ones are at least lower by an order of magnitude because of the smaller CKM matrix elements. The obtained distribution for the various components contributions to the considered decays can be tested by future experimental measurements. Additionally, our predictions on the $\chi_{c1}(2P)$ modes could help to understand the $X(3872)$ properties.

Acknowledgments

This work is supported by National Natural Science Foundation of China under Grants No.12075086 and No.11605060 and the Natural Science Foundation of Hebei Province under Grants No.A2021209002 and No.A2019209449.

Appendix A: DETAILS FOR DERIVING $\chi_{c1}(2P)$ CHARMONIUM DAS

We begin with the momentum-space radial wave function which can be written as Fourier transform of the position-space expression $\Psi_{nlm}(\vec{r})$

$$\Psi(k) = \int_{-\infty}^{\infty} \Psi_{nlm}(\vec{r}) e^{-\vec{k}\cdot\vec{r}} d\vec{r}, \quad (\text{A1})$$

where n , l , and m stand for main, orbital, and magnetic quantum numbers, respectively. In the spherical coordinates (r, θ, φ) , The two terms $\Psi_{nlm}(\vec{r})$ and $e^{-\vec{k}\cdot\vec{r}}$ in Eq. (A1) can be written as

$$\begin{aligned} \Psi_{nlm}(\vec{r}) &= R_{nl}(r) Y_{lm}(\theta, \varphi), \\ e^{-\vec{k}\cdot\vec{r}} &= e^{-ikr \cos \theta} = \sum_{l'=0}^{\infty} \sqrt{4\pi(2l'+1)} (-i)^{l'} j_{l'}(kr) Y_{l'0}(\theta, 0), \end{aligned} \quad (\text{A2})$$

with $j_{l'}(kr)$ is the spherical Bessel function. Substituting the results Eq. (A2) in Eq. (A1), we obtain

$$\Psi(k) = \sqrt{4\pi(2l'+1)} (-i)^l \int_0^{\infty} j_l(kr) R_{nl} r^2 dr, \quad (\text{A3})$$

where the orthogonality property $\int_0^{\pi} \int_0^{2\pi} Y_{lm} Y_{l'm'} \sin \theta d\theta d\varphi = \delta_{ll'} \delta_{mm'}$ have been employed. For the $\chi_{c1}(2P)$ state with quantum numbers $n = 3$ and $l = 1$, employing the spherical Bessel function $j_1(kr) = \frac{\sin(kr) - kr \cos(kr)}{(kr)^2}$ and the radial wave function for a Coulomb Potential $R_{31}(r) \propto r \left(1 - \frac{q_B r}{6}\right) e^{-\frac{1}{3} q_B r}$ with q_B being the Bohr momentum. The integral of Eq.(A3) evaluates to

$$\Psi(k) \propto \frac{k(9k^2 - q_B^2)}{(q_B^2 + 9k^2)^4}. \quad (\text{A4})$$

Following the similar strategy proposed in Refs. [50, 120], we obtain the heavy quarkonium DA which is dependent on the charm quark momentum fraction x after integrating the transverse momentum k_T ,

$$\Phi(x) \sim \int d^2 k_T \Psi(x, k_T) \propto x(1-x) \times \left\{ \frac{((1-2x)^2(1-x)x)^{3/2}}{\left(1 - \frac{4}{9}(v^2-9)(x-1)x\right)^3} \right\}, \quad (\text{A5})$$

where $v = q_B/m_c$ is the charm quark velocity. Similar to the DAs of $\chi_{c1}(1P)$ [84], we can propose that of $\chi_{c1}(2P)$ as $\Psi(x) \propto \Phi_{asy}(x) \mathcal{T}(x)$ with

$$\mathcal{T}(x) = \left\{ \frac{((1-2x)^2(1-x)x)^{3/2}}{\left(1 - \frac{4}{9}(v^2-9)(x-1)x\right)^3} \right\}^{1-v^2}, \quad (\text{A6})$$

where the power $1 - v^2$ denotes the small relativistic corrections to the Coulomb wave functions. In the numerical calculation, we take $v^2 = 0.3$ for charmonium [120]. The asymptotic forms of $\Phi_{asy}(x)$ depends on the corresponding twists for $\chi_{c1}(2P)$.

-
- [1] Particle Data Group, Review of particle physics, Prog. Theor. Exp. Phys. 2020, 083C01 (2020).
 - [2] R. Kumar *et al.* (Belle Collaboration), Observation of $B^{\pm} \rightarrow \chi_{c1} \pi^{\pm}$ and Search for Direct CP Violation, Phys. Rev. D **74**, 051103 (2006).
 - [3] R. Kumar *et al.* (Belle Collaboration), Evidence for $B^0 \rightarrow \chi_{c1} \pi^0$ at Belle, Phys. Rev. D **78**, 091104 (2008).
 - [4] N. Soni *et al.* (Belle Collaboration), Measurement of branching fractions for $B \rightarrow \chi_{(c1(2))} K(K^*)$ at BELLE, Phys. Lett. B **634**, 155 (2006).
 - [5] K. Abe *et al.* (Belle Collaboration), Observation of $\chi_{(c2)}$ production in B meson decay. Phys. Rev. Lett. **89**, 011803 (2002).
 - [6] B. Aubert *et al.* (BABAR Collaboration), Measurement of branching fractions and charge asymmetries for exclusive B decays to charmonium. Phys. Rev. Lett. **94**, 141801 (2005).

- [7] R. Mizuk *et al.* (Belle Collaboration), Observation of two resonancelike structures in the $\pi^+\chi_{c1}$ mass distribution in exclusive $\bar{B}^0 \rightarrow K^-\pi^+\chi_{c1}$ decays, Phys. Rev. D **78**, 072004 (2008).
- [8] R. Aaij *et al.* (LHCb Collaboration), Observation of the decay $\bar{B}_s^0 \rightarrow \chi_{c2}K^+K^-$ in the ϕ mass region, J. High Energy Phys. **08** (2018) 191.
- [9] V. Bhardwaj *et al.* (Belle Collaboration), Inclusive and exclusive measurements of B decays to χ_{c1} and χ_{c2} at Belle, Phys. Rev. D **93**, 052016 (2016).
- [10] S. Choi *et al.* (Belle Collaboration), Diquark-Antidiquark Interpretation of Mesons, Phys. Rev. Lett. **91**, 262001 (2003).
- [11] D. Acosta *et al.* (CDF Collaboration), Observation of the narrow state $X(3872) \rightarrow J/\psi\pi^+\pi^-$ in $p\bar{p}$ collisions at $\sqrt{s} = 1.96$ TeV, Phys. Rev. Lett. **93**, 072001 (2004).
- [12] V. Abazov *et al.* (D0 Collaboration), Observation and properties of the $X(3872)$ decaying to $J/\psi\pi^+\pi^-$ in $p\bar{p}$ collisions at $\sqrt{s} = 1.96$ TeV, Phys. Rev. Lett. **93**, 162002 (2004).
- [13] B. Aubert *et al.* (BABAR Collaboration), Study of the $B \rightarrow J/\psi K^-\pi^+\pi^-$ decay and measurement of the $B \rightarrow X(3872)K^-$ branching fraction, Phys. Rev. D **71**, 071103 (2005).
- [14] R. Aaij *et al.* (LHCb Collaboration), Observation of $X(3872)$ production in pp collisions at $\sqrt{s} = 7$ TeV, Eur. Phys. J. C **72**, 1972 (2012).
- [15] A. Bala *et al.* (Belle Collaboration), Observation of $X(3872)$ in $B \rightarrow X(3872)K\pi$ decays, Phys. Rev. D **91**, 051101 (2015).
- [16] S.-K. Choi *et al.* (Belle Collaboration), Bounds on the width, mass difference and other properties of $X(3872) \rightarrow \pi^+\pi^-J/\psi$ decays, Phys. Rev. D **84**, 052004 (2011).
- [17] A. Abulencia *et al.* (CDF Collaboration), Analysis of the Quantum Numbers J^{PC} of the $X(3872)$, Phys. Rev. Lett. **98**, 132002 (2007).
- [18] R. Aaij *et al.* (LHCb Collaboration), Determination of the $X(3872)$ Meson Quantum Numbers, Phys. Rev. Lett. **110**, 222001 (2013).
- [19] R. Aaij *et al.* (LHCb Collaboration), Quantum numbers of the $X(3872)$ state and orbital angular momentum in its $\rho^0 J/\psi$ decay, Phys. Rev. D **92**, 011102 (2015).
- [20] S. Chatrchyan *et al.* (CMS Collaboration), Measurement of the $X(3872)$ Production Cross Section Via Decays to $J/\psi\pi^+\pi^-$ in pp collisions at $\sqrt{s} = 7$ TeV, J. High Energy Phys. **04** (2013) 154.
- [21] A. Abulencia *et al.* (CDF Collaboration), Measurement of the Dipion Mass Spectrum in $X(3872) \rightarrow J/\psi\pi^+\pi^-$ Decays, Phys. Rev. Lett. **96**, 102002 (2006).
- [22] ATLAS Collaboration, Measurements of $\psi(2S)$ and $X(3872) \rightarrow J/\psi\pi^+\pi^-$ production in pp collisions at $\sqrt{s} = 8$ TeV with the ATLAS detector, J. High Energy Phys. **01** (2017) 117.
- [23] R. Aaij *et al.* (LHCb Collaboration), Observation of Multiplicity Dependent Prompt $\chi_{c1}(3872)$ and $\psi(2S)$ Production in pp Collisions, Phys. Rev. Lett. **126**, 092001 (2021).
- [24] R. Aaij *et al.* (LHCb Collaboration), Study of the lineshape of the $\chi_{c1}(3872)$ state, Phys. Rev. D **102**, 092005 (2020).
- [25] R. Aaij *et al.* (LHCb Collaboration), Study of the $\psi_2(3823)$ and $\chi_{c1}(3872)$ states in $B^+ \rightarrow (J/\psi\pi^+\pi^-)K^+$ decays, J. High Energy Phys. **08** (2020) 123.
- [26] N.N. Achasov and E.V. Rogozina, $X(3872)$, $I^G(J^{PC}) = 0^+(1^{++})$, as the $\chi_{c1}(2P)$ charmonium, Mod. Phys. Lett. A **30**, 1550181 (2015).
- [27] N.A. Tornqvist, Isospin breaking of the narrow charmonium state of Belle at 3872 MeV as a deuson, Phys. Lett. B **590**, 209 (2004).
- [28] E.S. Swanson, Short range structure in the $X(3872)$, Phys. Lett. B **588**, 189 (2004).
- [29] C.-Y. Wong, Molecular states of heavy quark mesons, Molecular states of heavy quark mesons, Phys. Rev. C **69**, 055202 (2004).
- [30] L. Maiani, F. Piccinini, A.D. Polosa and V. Riquer, Diquark-antidiquarks with hidden or open charm and the nature of $X(3872)$, Phys. Rev. D **71**, 014028 (2005).
- [31] B.A. Li, Is $X(3872)$ a possible candidate of hybrid meson? , Phys. Lett. B **605**, 306 (2005).
- [32] K.K. Seth, An alternative interpretation of $X(3872)$, Phys. Lett. B **612**,1 (2005).
- [33] R.D. Matheus, F.S. Navarra, M. Nielsen and C.M. Zanetti, QCD sum rules for the $X(3872)$ as a mixed molecule-charmonium state, Phys. Rev. D **80**, 056002 (2009).
- [34] M. Suzuki, The $X(3872)$ boson: Molecule or charmonium, Phys. Rev. D **72**, 114013 (2005).
- [35] Y. S. Kalashnikova, Coupled-channel model for charmonium levels and an option for $X(3872)$, Phys. Rev. D **72**, 034010 (2005).
- [36] M. Takizawa and S. Takeuchi, $X(3872)$ as a hybrid state of charmonium and the hadronic molecule, PTEP **2013**, 093D01 (2013).
- [37] W. Chen, H.-y. Jin, R.T. Kleiv, T.G. Steele, M. Wang and Q. Xu, QCD sum-rule interpretation of $X(3872)$ with $J^{PC} = 1^{++}$ mixtures of hybrid charmonium and molecular currents, Phys. Rev. D **88**, 045027 (2013).
- [38] P. C.Wallbott, G. Eichmann, and C. S. Fischer, $X(3872)$ as a four-quark state in a Dyson-Schwinger/Bethe-Salpeter approach, Phys. Rev. D **100**, 014033 (2019).
- [39] R. D. Matheus, S. Narison, M. Nielsen, and J. M. Richard, Can the $X(3872)$ be a 1^{++} four-quark state? , Phys. Rev. D **75**, 014005 (2007).
- [40] S. Dubnicka, A. Z. Dubnickova, M. A. Ivanov, and J. G. Korner, Quark model description of the tetraquark state $X(3872)$ in a relativistic constituent quark model with infrared confinement, Phys. Rev. D **81**, 114007 (2010).
- [41] P. Colangelo, F. De Fazio, and S. Nicotri, $X(3872) \rightarrow D\bar{D}\gamma$ decays and the structure of $X(3872)$, Phys. Lett. B **650**, 166 (2007).
- [42] M. Butenschoen, Z.-G. He, and B. A. Kniehl, Deciphering the $X(3872)$ via its polarization in prompt production at the

- CERN LHC, Phys. Rev. Lett. **123**, 032001 (2019).
- [43] S. Coito, G. Rupp, and E. van Beveren, $X(3872)$ is not a true molecule, Eur. Phys. J. C **73**, 2351 (2013).
- [44] S. L. Olsen, T. Skwarnicki, and D. Zieminska, Nonstandard heavy mesons and baryons: Experimental evidence, Rev. Mod. Phys. **90**, 015003 (2018).
- [45] Blaženka Melić, LCSR analysis of exclusive two body B decay into charmonium, Phys. Lett. B **591**, 91 (2004).
- [46] Z.-Z. Song, K.-T. Chao, Problems of QCD factorization in exclusive decays of B meson to charmonium, Phys. Lett. B **568**, 127 (2003).
- [47] Z.-Z. Song, C. Meng, Y.-J. Gao, K.-T. Chao, Infrared divergences of B meson exclusive decays to P wave charmonia in QCD factorization and nonrelativistic QCD, Phys. Rev. D **69**, 054009 (2004).
- [48] M. Beneke, F. Maltoni, and I. Z. Rothstein, QCD analysis of inclusive B decay into charmonium, Phys. Rev. D **59**, 054003 (1999).
- [49] M. Beneke, and L. Vernazza, $B \rightarrow \chi_{cJ}K$ decays revisited, Nucl. Phys. **B811**, 155 (2009).
- [50] C.-H. Chen, H.-N. Li, Nonfactorizable contributions to B meson decays into charmonia, Phys. Rev. D **71**, 114008 (2005).
- [51] Z. Rui, Q. Zhao, and L. Zhang, Branching ratios and CP asymmetries of $B \rightarrow \chi_{c1}K(\pi)$ decays, Eur. Phys. J. C **78**, 463 (2018).
- [52] C. Meng, Y.J. Gao, K.T. Chao, $B \rightarrow \chi_{c1}(1P, 2P)K$ decays in QCD factorization and $X(3872)$, Phys. Rev. D **87**, 074035 (2013).
- [53] X. Liu, Y. M. Wang, Revisiting $B^+ \rightarrow X(3872) + K^+$ in pQCD assigning to $X(3872)2^3P_1$ charmonium, Eur. Phys. J. C **49**, 643 (2007).
- [54] Y. Kato *et al.* (Belle Collaboration), Measurements of the absolute branching fractions of $B^+ \rightarrow X_{cc}K^+$ and $B^+ \rightarrow \bar{D}^{(*)0}$ at Belle, Phys. Rev. D **97**, 012005 (2018).
- [55] S. X. Nakamura, “Triangle singularities in $\bar{B}^0 \rightarrow \chi_{c1}K^-\pi^+$ relevant to $Z_1(4050)$ and $Z_2(4250)$,” Phys. Rev. D **100**, 011504 (2019).
- [56] S. X. Nakamura and K. Tsushima, “ $Z_c(4430)$ and $Z_c(4200)$ as triangle singularities,” Phys. Rev. D **100**, 051502 (2019).
- [57] S. X. Nakamura, “ $Z_c(4430)$, $Z_c(4200)$, $Z_1(4050)$, and $Z_2(4250)$ as triangle singularities,” AIP Conf. Proc. **2249**, 030006 (2020).
- [58] W. F. Wang, H. n. Li, W. Wang and C. D. Lü, S -wave resonance contributions to the $B_{(s)}^0 \rightarrow J/\psi\pi^+\pi^-$ and $B_s \rightarrow \pi^+\pi^-\mu^+\mu^-$ decays, Phys. Rev. D **91**, 094024 (2015).
- [59] Z. Rui, and W. F. Wang, S -wave $K\pi$ contributions to the hadronic charmonium B decays in the perturbative QCD approach, Phys. Rev. D **97**, 033006 (2018).
- [60] Z. Rui, Y. Li, and H. N. Li, P -wave contributions to $B \rightarrow \psi\pi\pi$ decays in perturbative QCD approach, Phys. Rev. D **98**, 113003 (2018).
- [61] Z. Rui, Y. Q. Li, and J. Zhang, Isovector scalar $a_0(980)$ and $a_0(1450)$ resonances in the $B \rightarrow \psi(K\bar{K}, \pi\eta)$ decays, Phys. Rev. D **99**, 093007 (2019).
- [62] Z. Rui, Y. Li, and Hong Li, Studies of the resonance components in the B_s decays into charmonia plus kaon pair, Eur. Phys. J. C **79**, 792 (2019).
- [63] Y. Li, D.-C. Yan, Z. Rui, Z.-J. Xiao, S , P and D -wave resonance contributions to $B_{(s)} \rightarrow \eta_c(1S, 2S)K\pi$ decays in the perturbative QCD approach, Phys. Rev. D **101**, 016015 (2020).
- [64] Y. Li, Z. Rui, and Z.-J. Xiao, P -wave contributions to $B_{(s)} \rightarrow \psi K\pi$ decays in perturbative QCD approach, Chin. Phys. C **44**, 073102 (2020).
- [65] Y. Li, A.-J. Ma, Z. Rui, and Z.-J. Xiao, Quasi-two-body decays $B \rightarrow \eta_c(1S, 2S) [\rho(770), \rho(1450), \rho(1700) \rightarrow] \pi\pi$ in the perturbative QCD approach, Nuc. Phys. **B924**, 745 (2017).
- [66] Z. Rui, Y. Li, and H. n. Li, Four-body decays $B_{(s)} \rightarrow (K\pi)_{S/P}(K\pi)_{S/P}$ in the perturbative QCD approach, J. High Energy Phys. **05** (2021) 082.
- [67] Y. Li, D. C. Yan, Z. Rui and Z. J. Xiao, Study of $B_{(s)} \rightarrow (\pi\pi)(K\pi)$ decays in the perturbative QCD approach, arXiv:2107.10684.
- [68] A. G. Grozin, On wave functions of meson pairs and meson resonances, Sov. J. Nucl. Phys. **38**, 289 (1983).
- [69] A. G. Grozin, One- and two-particle wave functions of multihadron systems, Theor. Math. Phys. **69**, 1109 (1986).
- [70] D. Müller, D. Robaschik, B. Geyer, F.-M. Dittes, and J. Hořejší, Wave functions, evolution equations and evolution kernels from light ray operators of QCD, Fortschr. Physik. **42**, 101 (1994).
- [71] M. Diehl, T. Gousset, B. Pire and O. Teryaev, Probing partonic structure in $\gamma^*\gamma \rightarrow \pi\pi$ near threshold, Phys. Rev. Lett. **81**, 1782 (1998).
- [72] M. Diehl, T. Gousset and B. Pire, Exclusive production of pion pairs in $\gamma^*\gamma$ collisions at large Q^{2*} , Phys. Rev. D **62**, 073014 (2000).
- [73] B. Pire and L. Szymanowski, Impact representation of generalized distribution amplitudes, Phys. Lett. B **556**, 129 (2003).
- [74] M.V. Polyakov, Hard exclusive electroproduction of two pions and their resonances, Nucl. Phys. B **555**, 231 (1999).
- [75] Y. Li, D. C. Yan, J. Hua, Z. Rui, and H. n. Li, Global determination of two-meson distribution amplitudes from three-body B decays in the perturbative QCD approach, arXiv: 2105.03899.
- [76] H. n. Li, QCD aspects of exclusive B meson decays, Prog. Part. Nucl. Phys. **51**, 85 (2003), and references therein.
- [77] H. n. Li and Y. M. Wang, Non-dipolar Wilson links for transverse-momentum-dependent wave functions, J. High Energy Phys. **06** (2015) 013.
- [78] H. n. Li, Y. L. Shen and Y. M. Wang, Next-to-leading-order corrections to $B \rightarrow \pi$ form factors in k_T factorization, Phys. Rev. D **85**, 074004 (2012).

- [79] T. Kurimoto, H. n. Li, and A. I. Sanda, Leading-power contributions to $B \rightarrow \pi, \rho$ transition form factors, Phys. Rev. D **65**, 014007 (2001).
- [80] J. Hua, H. n. Li, C. D. Lü, W. Wang, and Zhi-Peng Xing, Global Analysis of hadronic two-body B decays in the perturbative QCD approach, arXiv: 2012.15074.
- [81] W. Wang, Y. M. Wang, J. Xu, and S. Zhao, B -meson lightcone distribution amplitude from the Euclidean quantity, Phys. Rev. D **102**, 011502 (2020).
- [82] H. n. Li and H. S. Liao, B meson wave function in k_T factorization, Phys. Rev. D **70**, 074030 (2004).
- [83] H. n. Li, Y. L. Shen and Y. M. Wang, Resummation of rapidity logarithms in B meson wave functions, J. High Energy Phys. **02** (2013) 008.
- [84] Z. Rui, Probing the P -wave charmonium decays of B_c meson, Phys. Rev. D **97**, 033001 (2018).
- [85] X. P. Wang and D. Yang, The leading twist light-cone distribution amplitudes for the S-wave and P-wave quarkonia and their applications in single quarkonium exclusive productions, J. High Energy Phys. **06** (2014) 121.
- [86] Y. Q. Li, M. K. Jia and Z. Rui, Revisiting nonfactorizable contributions to factorization-forbidden decays of B mesons to charmonium, Chin. Phys. C **44**, 113104 (2020).
- [87] C. H. Chen, and H. N. Li, Three body nonleptonic B decays in perturbative QCD, Phys. Lett. B **561**, 258 (2003).
- [88] H.-Y. Cheng, C.-K. Chua, and K.-C. Yang, Charmless hadronic B decays involving scalar mesons: Implications on the nature of light scalar mesons, Phys. Rev. D **73**, 014017 (2006).
- [89] H.-Y. Cheng, C.-K. Chua, and K.-C. Yang, Charmless B decays to a scalar meson and a vector meson, Phys. Rev. D **77**, 014034 (2008).
- [90] S. Stone and L. Zhang, Use of $B \rightarrow J/\psi f_0$ decays to discern the $q\bar{q}$ or tetraquark nature of scalar mesons, Phys. Rev. Lett. **111**, 062001 (2013).
- [91] R. Fleischer, R. Knegjens and G. Ricciardi, Anatomy of $B_{s,d}^0 \rightarrow J/\psi f_0(980)$, Eur. Phys. J. C **71**, 1832 (2011).
- [92] R. L. Jaffe, Exotica, Phys. Rept. **409**, 1 (2005).
- [93] E. Klempt and A. Zaitsev, Glueballs, Hybrids, Multiquarks. Experimental facts versus QCD inspired concepts, Phys. Rept. **454**, 1 (2007).
- [94] R. Aaij *et al.* (LHCb Collaboration), Measurement of resonant and CP components in $\bar{B}_s^0 \rightarrow J/\psi \pi^+ \pi^-$ decays, Phys. Rev. D **89**, 092006 (2014).
- [95] A.-J. Ma, Y. Li, W. F. Wang and Z.-J. Xiao, S -wave resonance contributions to the $B_{(s)}^0 \rightarrow \eta_c(2S) \pi^+ \pi^-$ in the perturbative QCD factorization approach, Chin. Phys. C **41**, 083105 (2017).
- [96] Y. Li, A.-J. Ma, W. F. Wang and Z.-J. Xiao, The S -wave resonance contributions to the three-body decays $B_{(s)}^0 \rightarrow \eta_c f_0(X) \rightarrow \eta_c \pi^+ \pi^-$ in perturbative QCD approach, Eur. Phys. J. C **76**, 675 (2016).
- [97] Z. Rui, Y. Li, and W. F. Wang, The S -wave resonance contributions in the B_s^0 decays into $\psi(2S, 3S)$ plus pion pair, Eur. Phys. J. C **77**, 199 (2017).
- [98] S. M. Flatté, On the Nature of 0^+ Mesons, Phys. Lett. B **63**, 228 (1976).
- [99] D. V. Bugg, The Mass of the sigma pole, J. Phys. G **34**, 151 (2007).
- [100] R. Aaij *et al.* (LHCb Collaboration), Dalitz plot analysis of $B^0 \rightarrow \bar{D}^0 \pi^+ \pi^-$ decays, Phys. Rev. D **92**, 032002 (2015).
- [101] R. Aaij *et al.* (LHCb Collaboration), Measurement of the CP-violating phase β in $B^0 \rightarrow J/\psi \pi^+ \pi^-$ decays and limits on penguin effects, Phys. Lett. B **742**, 38 (2015).
- [102] R. Aaij *et al.* (LHCb Collaboration), Measurement of the resonant and CP components in $\bar{B}^0 \rightarrow J/\psi \pi^+ \pi^-$ decays, Phys. Rev. D **90**, 012003 (2014).
- [103] J. R. Pelaez, From controversy to precision on the sigma meson: a review on the status of the non-ordinary $f_0(500)$ resonance, Phys. Rept. **658**, 1 (2016).
- [104] J. A. Oller, Final state interactions in hadronic D decays, Phys. Rev. D **71**, 054030 (2005).
- [105] R. Aaij *et al.* (LHCb Collaboration), Amplitude analysis of the $B^+ \rightarrow \pi^+ \pi^+ \pi^-$ decay, Phys. Rev. D **101**, 012006 (2020).
- [106] H. Y. Cheng, C. W. Chiang and C. K. Chua, Finite-Width Effects in Three-Body B Decays, Phys. Rev. D **103**, 036017 (2021).
- [107] D. Aston *et al.* (LASS Collaboration), A study of $K^- \pi^+$ scattering in the reaction $K^- p \rightarrow K^- \pi^+$ at 11GeV/c, Nucl. Phys. **B296**, 493 (1988).
- [108] B. Aubert *et al.* (BaBar Collaboration), Dalitz-plot analysis of the decays $B^\pm \rightarrow K^\pm \pi^\mp \pi^\pm$, Phys. Rev. D **72**, 072003 (2005).
- [109] B. Aubert *et al.* (BaBar Collaboration), Dalitz-plot analysis of the decays $B^\pm \rightarrow K^\pm \pi^\mp \pi^\pm$, Phys. Rev. D **74**, 099903 (2006).
- [110] D. V. Bugg, Re-analysis of data on $a(0)(1450)$ and $a(0)(980)$, Phys. Rev. D **78**, 074023 (2008).
- [111] Z. Rui, Y. Li, and Zhen-Jun Xiao, Branching ratios, CP asymmetries and polarizations of $B \rightarrow \psi(2S)V$ decays, Eur. Phys. J. C **77**, 610 (2017).
- [112] H.-N. Li and B. Melic, Determination of heavy meson wave functions from B decays, Eur. Phys. J. C **11**, 695 (1999).
- [113] M. Beneke, G. Buchalla, M. Neubert and C.T. Sachrajda, QCD factorization for $B \rightarrow \pi\pi$ decays: Strong phases and CP violation in the heavy quark limit, Phys. Rev. Lett. **83**, 1914 (1999).
- [114] M. Beneke, G. Buchalla, M. Neubert and C. T. Sachrajda, QCD factorization for exclusive, nonleptonic B meson decays: General arguments and the case of heavy light final states, Nucl. Phys. B **591**, 313 (2000).
- [115] M. Beneke, G. Buchalla, M. Neubert and C. T. Sachrajda, QCD factorization in $B \rightarrow \pi K, \pi\pi$ decays and extraction of Wolfenstein parameters, Nucl. Phys. B **606**, 245 (2001).
- [116] B. Aubert *et al.* (BaBar Collaboration), Search for the $Z(4430)^-$ at BABAR, Phys. Rev. D **79**, 112001 (2009).

- [117] J. P. Lees *et al.* (BaBar Collaboration), Search for the $Z_1(4050)^+$ and $Z_2(4250)^+$ states in $\bar{B}^0 \rightarrow \chi_{c1} K^- \pi^+$ and $B^+ \rightarrow \chi_{c1} K_S^0 \pi^+$, Phys. Rev. D **85**, 052003 (2012).
- [118] B. Aubert *et al.* (BaBar Collaboration), Dalitz plot analysis of the decay $B^\pm \rightarrow K^\pm K^\pm K^\mp$, Phys. Rev. D **74**, 032003 (2006).
- [119] M. Ablikim *et al.* (BES Collaboration), Partial wave analysis of $\chi_{c0} \rightarrow \pi^+ \pi^- K^+ K^-$, Phys. Rev. D **72**, 092002 (2005).
- [120] A. E. Bondar and V. L. Chernyak, Is the BELLE result for the cross section $\sigma(e^+ e^- \rightarrow J/\psi + \eta_c)$ a real difficulty for QCD? , Phys. Lett. B **612**, 215 (2005).